CSCanada
Energy Science and Technology
Vol. 3, No. 2, 2012, pp. 10-17
DOI:10.3968/j.est.1923847920120302.263

ISSN 1923-8460[PRINT]
ISSN 1923-8479[ONLINE]
www.cscanada.net
www.cscanada.org

Superstrate $CuInSe_2$-Printed Solar Cells on In_2S_3/TiO_2/FTO/Glass Plates

Duy-Cuong Nguyen[a]; Seigo Ito[a], *; Masamichi Inoue[b]; Shin-ichi Yusa[b]

[a]Department of Electrical Engineering and Computer Sciences, Graduate School of Engineering, University of Hyogo, 2167 Shosha, Himeji, Hyogo 671-2280, Japan.
[b]Department of Materials Science and Chemistry, Graduate School of Engineering, University of Hyogo, 2167 Shosha, Himeji, Hyogo 671-2280, Japan.
*Corresponding author.

Funded by the Innovative Solar Cells project (NEDO, Japan).

Received 3 February 2012; accepted 18 April 2012

Abstract

$CuInSe_2$ powders synthesized by ball milling were printed on In_2S_3/TiO_2/FTO/glass substrates, resulting in superstrate solar cells. Although particle structure of $CuInSe_2$ in the layer remained after heating at 600 °C under N_2 gas, photovoltaic effects were observed; the open-circuit voltage and short-circuit current density were 0.45 V and 5.6 mA/cm^2, respectively. The effects of annealing time on the structural, optical and photovoltaic properties of $CuInSe_2$ were studied by scanning electron micrograph (SEM), X-ray diffraction (XRD), thermogravimetric analysis (TGA) and UV-Vis reflectance absorption spectroscopy. The $CuInSe_2$ solar cells were printed in air ambient without vacuum processing and without toxic and explosive chemicals (e.g., hydrazine, H_2Se and H_2S), which can offer a promising strategy for future research and industrial investigation into cost-effective photovoltaic systems.

Key words: Photovoltaic system; Photovoltaic effects; $CuInSe_2$ solar cells

Nguyen, D. C., Ito, S., Inoue, M., & Yusa, S. I. (2012). Superstrate $CuInSe_2$-Printed Solar Cells on In_2S_3/TiO_2/FTO/Glass Plates. *Energy Science and Technology*, *3*(2), 10-17. Available from: URL: http://www.cscanada.net/index.php/est/article/view/10.3968/j.est.1923847920120302.263
DOI: http://dx.doi.org/10.3968/j.est.1923847920120302.263

INTRODUCTION

The present photovoltaic system is too expensive to be a renewable generation resource. Therefore, without govemental supports (feed-in-tariffs[1], etc), the photovoltaic system can't produce the profit from the solar irradiation. Therefore, cost-effective solar-generation systems are necessary for future renewable energy. Chalcopyrite thin-film solar cells such as $CuInS_2$, $CuInSe_2$ and $Cu(In,Ga)Se_2$ are potential candidates for renewable energy power sources, owing to their high conversion efficiency ($CuInS_2$: 12.5%[2]; $CuInSe_2$: 14%[3]; $Cu(In,Ga)Se_2$:19.9%[4]). The structure of conventional chalcopyrite thin-film solar cells is <Mo (on glass substrate or Mo foil) / chalcopyrite (CIS, CISe or CIGSe) layer/ buffer layer (CdS or ZnS) / transparent-conductive-oxides (TCO) layer>, which is called as "substrate structure". "Substrate" and "superstrate" solar cells indicate solar cell structures fabricated on metal (non-photon transmitting) and transparent-conducting-oxide substrates, respectively.

As noted above, the substrate structure has been utilized for conventional chalcopyrite solar cells[2-5]. On the other hand, the superstrate structure has been utilized for thin-film Si[6], CdTe/CdS[7], dye-sensitized[8] and special chalcopyrite[9] solar cells. In conventional chalcopyrite thin-film solar cells, the <chalcopyrite layer/ buffer layer> interface must be smooth, flat and conformal, because the chalcopyrite layer must make good electrical contact with the very thin buffer layer (ca. 50 nm) to generates charge separation from excitons, and this interface prevents short-circuited contacts between the chalcopyrite layer and the TCO layer. Moreover, if the chalcopyrite layer consists of 1-μm particles, the TCO layer on the chalcopyrite layer cannot be continuous, resulting in no conductivity. Because of the necessity of such a smooth surface, powdery and rough layers have not been used in chalcopyrite solar cells.

In order to make conformal, compact and smooth chalcopyrite layers, which have been necessary for

fabrication of high-efficiency solar cells, annealing in H_2Se and H_2S gases or Se and S vapors (selenization and sulfurization) has been necessary; otherwise, the chalcopyrite layers were not photoactive. These layers can be fabricated by vacuum methods (evaporation and sputtering of Cu, In and Ga metals[4, 5, 10-12]) or non-vacuum methods (printing[13, 14], spray[15] and electrochemical deposition[16]). However, solar cells produced by selenization and sulfurization methods are expensive because of high-cost equipment and low-speed processing. Other drawbacks to selenization and sulfurization methods are the toxicity, reactivity and explosiveness of H_2Se and H_2S gases or Se and S vapors. One alternative is the spin-coating method developed by IBM[17, 18]. This IBM method can fabricate a flat layer of chalcopyrite, but highly toxic hydrazine, which should be eliminated, is used as the spin-coating solvent.

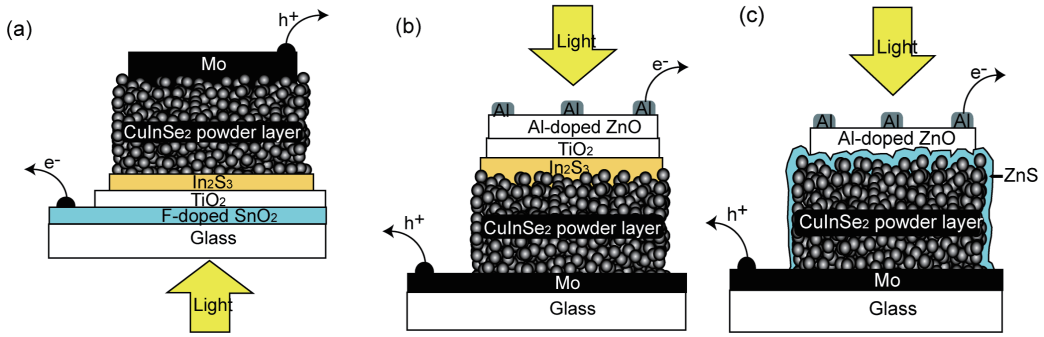

Figure 1
Structure of $CuInSe_2$-Printed Solar Cells: (a) Superstrate and (b, c) Substrate Structures. Thickness of Layers: TiO_2 (200 nm), In_2S_3 (100 nm), $CuInSe_2$ (30 μm), Mo (500 nm), ZnS (100 nm), Al-doped ZnO (500 nm) and Al (300 nm)

This is the first report of chalcopyrite-printed solar cells without utilization of hazards materials: H_2S, H_2Se, not hydrazine. The photovoltaic effects have been found using rough $CuInSe_2$ layers consisting of micron-sized $CuInSe_2$ powders on <In_2S_3/TiO_2/FTO/glass plate> only in a superstrate structure (Figure 1a). In this case, the layers of <In_2S_3/TiO_2> can serve as a buffer layer. The micron-sized $CuInSe_2$ particle synthesized by ball milling were printed on <In_2S_3/TiO_2/FTO/glass plate> under air ambient without vacuum processing and without toxic or explosive gas (e.g., H_2Se and H_2S). Although the particle structure of $CuInSe_2$ in the layer remained after heating at 600 °C for 1 min under N_2 gas, the open-circuit voltage and short-circuit current density were 0.45 V and 5.6 mA / cm^2, respectively. The effects of annealing time on structural, optical and photovoltaic properties of $CuInSe_2$ were discussed. This fabrication method of $CuInSe_2$-printed solar cells using less toxic material (without H_2Se, H_2S, and hydrazine) without no vacuum system offers a promising new strategy for future research and industrial investigation into cost-effective printed photovoltaic systems.

1. EXPERIMENTAL

$InCl_3$ (98%, Kishida Chemical Co., Ltd), thiourea (Tokyo Chemical Industry Co., Ltd), titanium isopropoxide (Kishida Chemical Co.), acetyl acetone (Kanto Chemical Co.), and ethanol (Kanto Chemical Co.) were utilized for buffer layer (TiO_2[19] and In_2Se_3[15]) fabrication by spray deposition on transparent conducting oxide substrates of florin-doped tin-oxide coated (FTO) glass plates (TEC7 t-2.2mm, Nippon Sheet Glass, Japan). Titanium isopropoxide was mixed with acetyl acetone (1/2: mol/mol) and the mixture was diluted ten times by ethanol for the spray solution to be TiO_2 layers. For In_2Se_3-sprayed layers, the aqueous solution with 10 mM $InCl_3$ and 20 mM thiourea was prepared. Both In_2S_3 and TiO_2 buffer layers were deposited by the spray method on a hot plate at 200 °C and 450 °C, resulting in the thicknesses of 100 nm and 300 nm, respectively. Before the In_2S_3 layer deposition, $TiCl_4$ (Kishida Chemical Co.) treatment[19] was performed in order to cap pinholes on spray-deposited TiO_2 layer.

The $CuInSe_2$ powder was synthesized from starting materials of Cu (99.9% purity, Wako), In (99.99% purity, Aldrich) and Se (99.9% purity, Nacalai Tesque) powders in a molar ratio of 1:1:2 by mechanical ball milling[13]. The milling process was performed in ambient air. To obtain a good $CuInSe_2$ phase, the parameters of mill processing (rotation speed and milling time) were optimized using XRD measurements. Changing the rotation speed, the XRD peak intensity was saturated at 700 rpm and XRD peak was shifted to that of $CuInSe_2$, 26.62 degree for (112) $CuInSe_2$ phase (Figure 2a)[20]. The additional rotation time can't improve the XRD intensity and pattern, moreover it produced the secondary phase at 31 degree in $CuInSe_2$ crystal which can deteriorate the PV performance (Figure 2b)[21]. The $CuInSe_2$ powder was mixture of submicron (small) particles and several micron (large) particles, confirmed by SEM (JEOL, JSM-6510) (Figure 3), which can't be changed by the mixing condition. The heating effect on the $CuInSe_2$ powder was studied using thermogravimetric analysis (TGA; EXSTAR6000, Seiko Instruments, Japan).

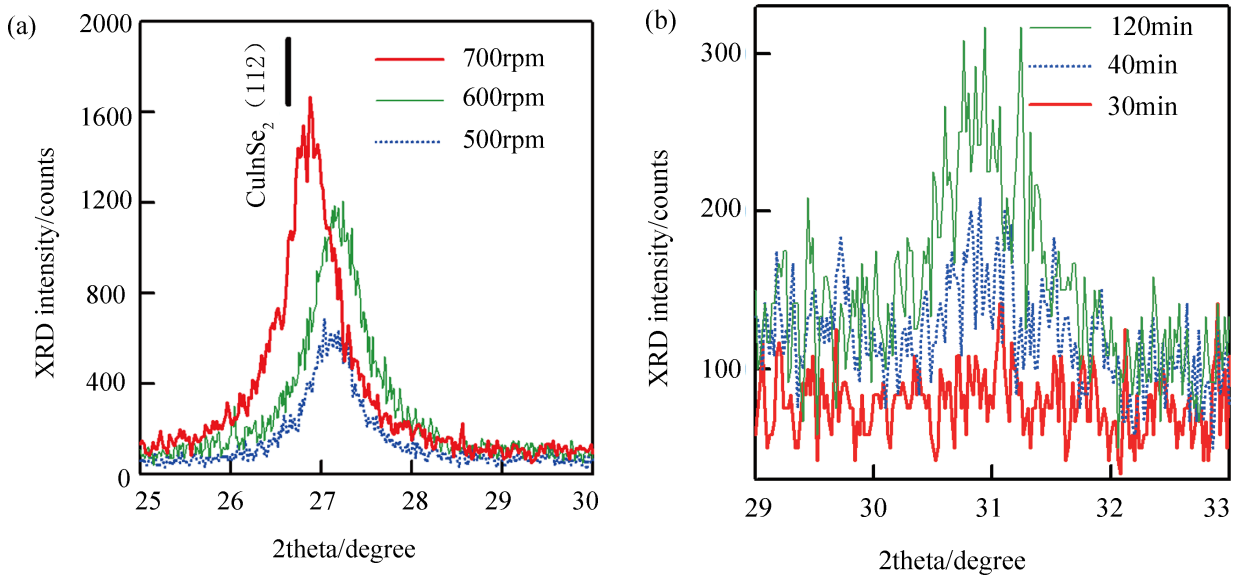

Figure 2
XRD Patterns $CuInSe_2$ Powders Prepared by Ball Milling for 30 min with Several Rotation Speeds (a) and with 700 rpm for Several Rotating Duration (b). The $CuInSe_2$ (112) Position at 26.625[18] was Shown in the Figure 2a as a Black Bar above the XRD Patterns.

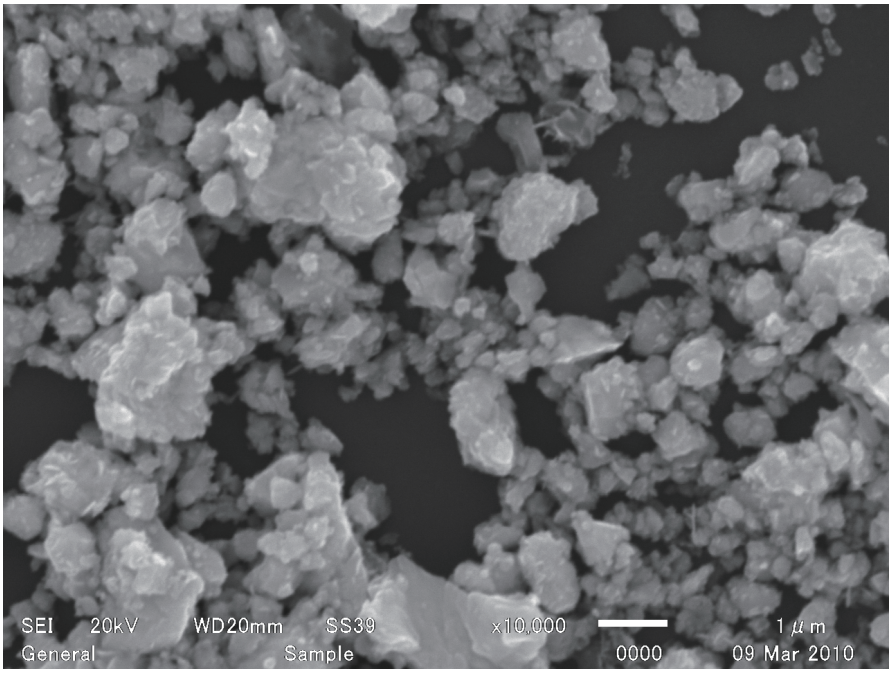

Figure 3
A SEM Image of $CuInSe_2$ Powder just after Preparation by Ball Milling at 700 rpm for 30 min

$CuInSe_2$ coating paste was prepared by mixing 0.7 g $CuInSe_2$ powder and 1 mL propylene glycol (Kanto Chemical Co.), and then grinding in a mortar. The $CuInSe_2$ layers were prepared by doctor blade printing on In_2S_3/TiO_2/FTO substrates. To improve the crystallinity of $CuInSe_2$ and remove defects, the $CuInSe_2$ samples should be annealed. Since selenium is easily evaporated from $CuInSe_2$ films if annealed for a long time, a short annealing time is necessary. Accordingly, rapid thermal annealing (RTA) was selected to anneal the $CuInSe_2$ films. The samples annealed at temperatures below 400 °C exhibited no change in the crystallinity or the microstructure of the films. In this paper, we show the results for the samples annealed at 600 °C because the effects of annealing time on the photovoltaic properties at this temperature were quite clear. After printing, hence,

the $CuInSe_2$ layer was dried at 125 °C for 30 min in air, and then annealed in a nitrogen atmosphere (1 atm) at 600 °C for 1, 2, 3 and 4 min.

The crystalline structure and the preferred orientation of the films were characterized by XRD (Rigaku Miniflex II) using CuK_α radiation. The thickness and microstructure of the films were viewed by SEM. Reflectance absorption spectra were measured by ultraviolet-visible spectroscopy (Lamda 750 UV/VIS Spectrometer, Perkin-Elmer). The area of samples for photocurrent-voltage measurement was 0.5 × 0.5 cm^2. Photovoltaic measurements used an AM 1.5 solar simulator equipped with a xenon lamp (YSS-100A,Yamashita Denso, Japan). The power of the simulated light was calibrated to 100 MW/cm^2 by using a reference Si photodiode (Bunkou Keiki Co. Ltd., Japan). Current-voltage curves were obtained by applying an external bias to the cell and measuring the generated photocurrent with a DC voltage current source (6240A, ADCMT, Japan).

In order to compare photovoltaic effects between superstrate- and substrate-structure printed solar cells, substrate-structured $CuInSe_2$-printedr solar cells were also fabricated (figure 1b and 1c). As shown in figure 1b, in place of a FTO layer, an Al-doped ZnO (AZO) layer, which was coated by sputtering deposition, was utilized for the transparent-conducting oxide (TCO) layer. It is very difficult to fabricate FTO layer on the $CuInSe_2$ layer, because FTO can be deposited by chemical vapor deposition on a high-temperature substrate (600 °C), which can decompose $CuInSe_2$ layer. About the buffer layer, a ZnS layer was also used (Figure 1c) in place of the $<TiO_2/In_2Se_3>$. The ZnS layer was fabricated by chemical bath deposition, and was a standard buffer layer for substrate-type chalcopyrite solar cells[22]. The reason why AZO was not used in figure 1a is that AZO is not stable under the printed solar cell procedure: acid treatment (dipping in $TiCl_4$ solution) and high-temperature spray deposition, resulting in deterioration of the AZO conductivity. On the other hand, FTO is very stable against heat and acid.

2. RESULTS AND DISCUSSIONS

2.1 Photovoltaic Results

The photovoltaic properties of superstrate and substrate solar cells are shown in figure 4. For the samples prepared on superstrates (Figure 1a), the short-circuit photocurrent and the open-circuit photovoltage decreased with increasing annealing time. Annealing time for 1 min provided the best photovoltaic results (short-circuit photocurrent density (J_{sc}): 5.6 $mAcm^{-2}$, open-circuit photovoltage (V_{oc}): 0.45 V, fill factor (*ff*): 0.27 and photoenergy conversion efficiency (η): 0.68%). The photocurrents were decreased for the sample annealed over 1 min. The reductive photovoltaic properties of $CuInSe_2$ films may arise from the instability of the In_2S_3 buffer layer at high temperatures, because In_2S_3 is not highly stable at temperatures above 400 °C[9]. In the case of substrate solar cells (Figure 1b and 1c), no photocurrent was observed, as shown in figure 2f and 2g, respectively.

2.2 Analysis of Materials

To analyze the microstructural properties of the $CuInSe_2$ films, the samples were observed by scanning electron microscopy (SEM). SEM cross-sectional images of samples prepared on substrates and annealed at 600 ºC for several minutes are shown in figure 5. It is difficult to determine the growth of grain size in the samples with increasing annealing time. Although the $CuInSe_2$ film was quite powdery, a substantial photocurrent was observed for these samples of superstrate-structured cells (Figure 4). On the other hand, substrate-structured cells produced no photovoltaic effect. The reason must be that the $CuInSe_2$ surface was too rough for substrate solar cells (Figure 1b and 1c), and consequently the buffer layer could not cover the entire cell area. Because of this problem, the leakage current increased and photocurrent was not observed for the $CuInSe_2$-printed substrate solar cells.

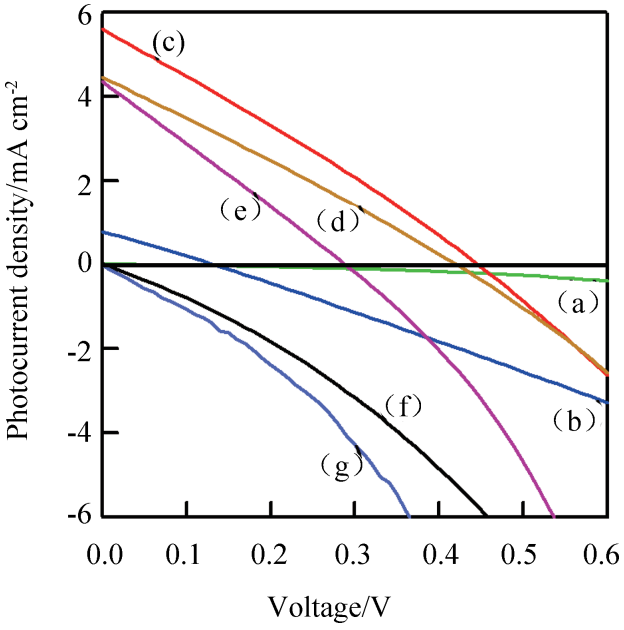

Figure 4

Photocurrent-Voltage Curves of Superstrate $CuInSe_2$-Printed Solar Cells Annealed at 600 °C for (a) 0, (b) 0.5, (c) 1, (d) 2 and (e) 3 min and Those of (f, g) Substrate $CuInSe_2$-Printed Solar Cells Annealed at 600 °C for 1 min, Corresponding to Figure 1(b) and Figure 1(c)

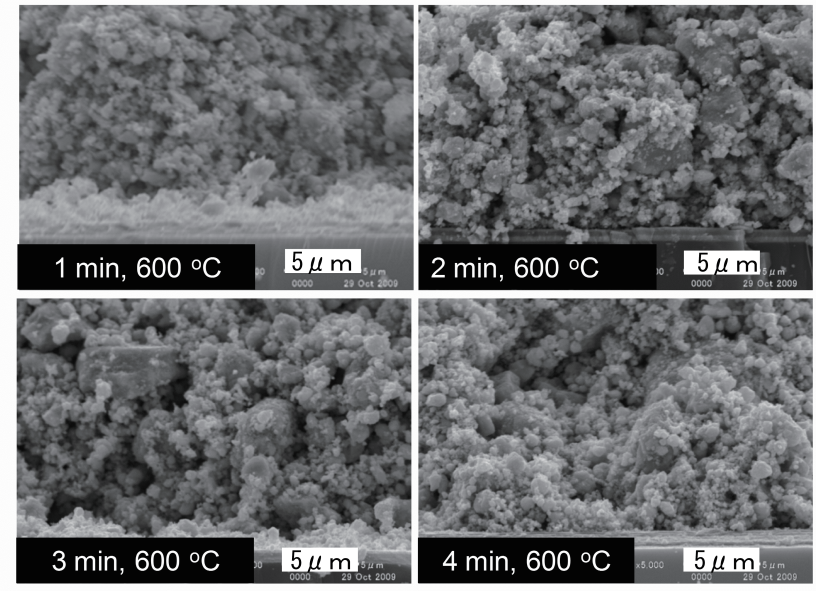

Figure 5
SEM Cross-Sectional Images of $CuInSe_2$-Printed Layer Annealed for 1, 2, 3 and 4 min

About the reason why the fill factor is only 0.27, which is lower than most of the CIGS solar cells reported in the literature, it may be due to the inter diffusion of In_2S_3 buffer layer to $CuInSe_2$ layer, resulting in the disappearance of electrical junction and in the decreasing of shunt resistance. Due to the low shunt resistance, the photovoltage became also low (0.45 V). In order to improve the photovoltaic effects, fabrication of thermal durable buffer layer is one of the important targets for the printed superstrate solar cells.

Although the $CuInSe_2$-printed solar cells produced the photovoltaic effects, the powder structure can be a drawback to improve the conversion efficiency. However, Shafarman and Zhu fabricated high-efficiency solar cells with small $Cu(InGa)Se_2$ grains; there was no simple correlation between grain size and device performance[23]. Hence, the further study and discussions are necessary about the effects of annealing time on the crystallinity of $CuInSe_2$. Figure 6a presents the XRD patterns of samples heated by RTA at 600 °C for 0, 1, 2, 3 and 4 min in a nitrogen atmosphere. The diffraction peaks for the annealed samples become sharper until 3 min. Heating at 3 min, a small shoulder at 26.4 degree can be observed. Heating at 4 min, the main peak of $CuInSe_2$ as (112) was shifted to 26.4 degree and the peak intensity become weaker. Since Cu_2Se crystal shows the peak at 26.4 degree as (111)[24], the shift of the $CuInSe_2$ (112) peak to 26.4 maybe suggests segregation of $CuInSe_2$ to Cu_2Se and In_2Se_3.

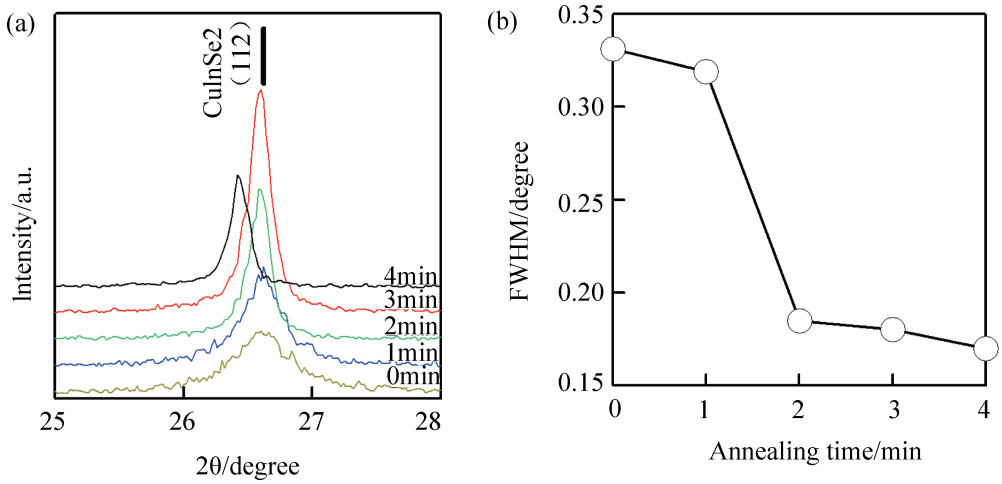

Figure 6
XRD Patterns (a) and the FWHM of (112) Orientation (b) of $CuInSe_2$-Printed Layers Annealed at 600 °C at 0, 1, 2, 3 and 4 min. The $CuInSe_2$ (112) Position at 26.625[18] was Shown in the Figure 6a as a Black Bar above the XRD Patterns.

As shown in figure 6b, the full width at half-maximum (FWHM) of the (112) peak become smaller with annealing duration, indicating growth of grain size. The change in FWHM from 1 min to 2 min is especially drastic. The decrease in the peak intensity may be due to the escape of selenium from the particle surface because the melting point of selenium is rather low (~217 °C)[25], resulting in the decomposition of small $CuInSe_2$ particles and enlargement of large $CuInSe_2$ particles. At the same time, the melting and evaporation of selenium attack the In_2S_3 buffer layer, resulting in the deterioration of photovoltaic effects (Figure 4). Moreover, we found the $CuInSe_2$ segregation to In_2Se_3 and Cu_2Se by XRD patterns by heating over 3 min (Figure 6a). Therefore, annealing the $CuInSe_2$ powder for 1 min was optimal for fabricating photovoltaic cells with better crystallinity and the better buffer layer condition.

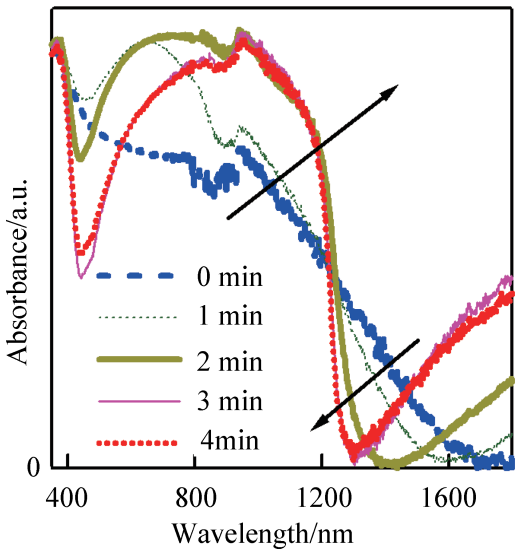

Figure 7
Reflectance Absorption Spectra of Printed $CuInSe_2$ Layer Annealed at 600 °C in Nitrogen Ambiance with Different Heating Time. Each Spectrum was Scaled at 380 nm Wavelength. The Arrows Show the Time Course with Heating Duration.

Reflectance absorption spectra of $CuInSe_2$ films annealed at 600 °C for several minutes are shown in figure 7, which are normalized at 350 nm. An isosbestic point was observed at 1240 nm. The slope of spectra increased with the annealing time until 3 min and saturated. The increased slope of the absorption spectra of the annealed samples can be attributed to the improved crystallinity of the $CuInSe_2$ films as XRD results (Figure 6). Band gap values calculated from absorption spectra for $CuInSe_2$ films annealed at 600 °C for 1, 2, 3 and 4 min are 0.706, 0.948, 0.993 and 0.993 eV, respectively. The value annealed for 2-4 min completely agrees with the reported band gap of the $CuInSe_2$ phase[26].

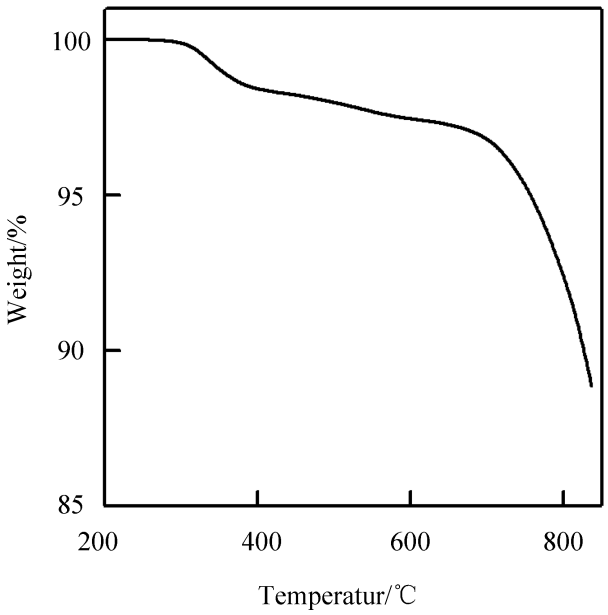

Figure 8
A Time Course Profile of Thermogravimetric Analysis (TGA) of $CuInSe_2$ Powder Prepared by Ball-Milling Method

In order to confirm the loss of selenium (discussed above), thermogravimetric analysis (TGA) of $CuInSe_2$ powder has been performed (Figure 8). The setting ramp-up temperature was 2 °C / min. The weight was decreased between 350-400 °C apparently. From 400 °C to 650 °C, the $CuInSe_2$ weight decreased steadily. Basically, $CuInSe_2$ crystal fabricated by vacuum method is very stable until 700 °C[27]. In this study, however, the weight of $CuInSe_2$ powder decreased steadily, which can be due to the loss of selenium from the surface of $CuInSe_2$ particles. Over 700°C, the $CuInSe_2$ weight decreased rapidly, which may be due to the evaporation of Se on the surface of $CuInSe_2$ particles, because the boiling point of Se is 685 °C.

CONCLUSIONS

In conclusion, $CuInSe_2$ solar cells were prepared by printing as substrate and superstrate structures without H_2S, H_2Se, and hydrazine. The crystallinity of $CuInSe_2$ films was considerably improved by annealing at 600 °C for several minutes in a nitrogen atmosphere. For the $CuInSe_2$ superstrate solar cells (Figure 1a), the $CuInSe_2$ absorption layers were powdery, but substantial photovoltaic effects were observed for 1 min heating at 600 °C: J_{sc}=5.6 m Acm^{-2}, V_{oc} = 0.45 V and η =0.68%. On the other hand, no photovoltaic effect was observed by the conventionally structured $CuInSe_2$ substrate solar cells (Figure 1b and 1c). In order to improve the conversion efficiency in the future work, it is very important to fabricate conformal flat $CuInSe_2$ layer. One of the ideas is to use smaller-sized particles for the layers, but the

$CuInSe_2$ particles can't melt at 600 °C without H_2Se gas (Figure 5). Therefore, the smaller-sized particles will not improve the conversion efficiency. Although the improvement of crystallinity has been confirmed after heating at 600 °C over 1 min, the photovoltaic effect has deteriorated because of the melting of buffer layer (In_2S_3) and the conversion of $CuInSe_2$ particle to Cu_2Se and In_2Se_3. The investigation of temperature-durable buffer layers is the future target for the printed $CuInSe_2$-powder solar cells to improve the conversion efficiency.

ACKNOWLEDGMENT

This work was funded by the Innovative Solar Cells project (NEDO, Japan).

REFERENCES

[1] Mendonca, M. (2007). *Feed-in Tariffs, Accelerating the Deployment of Renewable Energy*. USA: Earthscan Ltd.

[2] Klaer, J., Bruns, J., Henninger, R., Siemer, K., Klenk, R., Ellmer, K., & Bräunig, D. (1998). Efficient $CuInS_2$ Thin-Film Solar Cells Prepared by a Sequential Process. *Semicond. Sci. & Technol.*, *13*(12),1456-1458.

[3] Zweigart, S., Sun, S. M., Bilger, G., & Shock, W. H. (1996). $CuInSe_2$ Film Growth Using Precursors Deposited at Low Temperature. *Sol. Energy Mater. & Sol. Cells*, *41/42*, 219-229.

[4] Repins, I., Contreras, M. A., Egaas, B., De Hart C., Scharf, J., Perkins, C. L., To, B., Noufi, R. (2008). 19.9%-Efficient ZnO/CdS/$CuInGaSe_2$ Solar Cell with 81.2% Fill Factor. *Progress in Photovoltaics: Research and Applications*, *16*(3), 235-239.

[5] M. A. Contreras, B. Egaas, K. Ramanathan, J. Hiltner, A. Swartzlander, F. Hasoon, R. Noufi (1999). Progress Toward 20% Efficiency in Cu(In,Ga)Se_2 Polycrystalline Thin-Film Solar Cells. *Progress in Photovoltaics: Research and Applications*, *7*(4), 311-316.

[6] Battaglia, C., Söderström, K., Escarré, J., Haug, F.-J., Dominé, D., Cuony, P., Boccard, M., Bugnon, G., Denizot, C., Despeisse, M., Feltrin, A., & Ballif, C. (2010). Efficient Light Management Scheme for Thin Film Silicon Solar Cells via Transparent Random Nanostructures Fabricated by Nanoimprinting. *Appl. Phys. Lett.*, *96*(21), 213504.

[7] Aramoto, T., Kumazawa, S., Higuchi, H., Arita, T., Shibutani, S., Nishio, T., Nakajima, J., Tsuji, M., Hanafusa, A., Hibino, T., Omura, K., Ohyama, H., & Murozono, M. (1997). 16.0% Efficient Thin-Film CdS/CdTe Solar Cells. *Jpn. J. Appl. Phys.*, *36*, 6304-6305.

[8] Bach, U., Lupo, D., Comte, P., Moser, J. E., Weissörtel, F., Salbeck, J., Spreitzer, H., & Grätzel, M. (1998). *Nature*, 395, 583-585.

[9] Nakada, T., Kume, T., & Kunioka, A. (1998). Superstrate-Type CuInSe2-Based Thin Film Solar Cells by a Low-Temperature Process Using Sodium Compounds. S*ol. Energy. Mater. Sol. Cells*, *50*(1-4), 97-103.

[10] Ramanathan, K., Teeter, G., Keane, J. C., & Noufi, R. (2005). Properties of High-Efficiency $CuInGaSe_2$ Thin Film Solar Cells. *Thin Solid Films*, *480/481*, 499-502.

[11] Deepa, K. G., Jayakrishinan, R., Vijayakumar, K. P., Kartha, C. S., & Ganesan, V. (2009). Sub-micrometer Thick $CuInSe_2$ Films for Solar Cells Using Sequential Elemental Evaporation. *Solar Energy*, *83*(7), 964-968.

[12] Song, H. K., Kim, S. G., Kim, H. J., Kim, S. K., Kang, K. W., Lee, J. C., & Yoon, K. H. (2003). Preparation of $CuIn_{1-x}Ga_xSe_2$ Thin Films by Sputtering and Selenization Process. *Sol. Energy Mater. Sol. Cells*, *75*(1-2), 145-153.

[13] Wada, T., Matsuo, Y., Nomura, S., Nakamura, Y., Miyamura, A., Chiba, Y., Yamada, A., & Konagai, M. (2006). Fabrication of Cu(In,Ga)Se_2 Thin Films by a Combination of Mechanochemical and Screen-Printing/ Sintering Processes. *Phys. Stat. Sol. (a)*, *203*(11), 2593-2597.

[14] Ahn, S. J., Kim, C. W., Yun, J. H., Gwak, J., Jeong, S., Ryu, B. H., & Yoon, K. H. (2010). $CuInSe_2$ (CIS) Thin Film Solar Cells by Direct Coating and Selenization of Solution Precursors. *J. Phys. Chem. C*, *114*(17), 8108-8113.

[15] Goossens, A., & Hofhuis, J. (2008). Spray-Deposited $CuInS_2$ Solar Cells. *Nanotechnology*, *19*(42), 424018.

[16] Lincot, D., Guillemoles, J. F., Taunier, S., Guimard, D., Sicx-Kurdi, J., Chaumont, A., Roussel, O., Ramdani, O., Hubert, C., Fauvarque, J. P., Bodereau, N., Parissi, L., Panheleux, P., Fanouillere, P., Naghavi, N., Grand, P. P., Benfarah, M., Mogensen, P., Kerrec, O. (2004). Chalcopyrite Thin Film Solar Cells by Electrodeposition. *Solar Energy*, *77*(6), 725-737.

[17] Mitzi, D. B., Yuan, M., Liu, W., Kellock, A. J., Chey, S. J., Deline, V., & Schrott, A. G. (2008). A High-Efficiency Solution-Deposited Thin-Film Photovoltaic Device. *Adv. Mater.*, *20*(19), 3657-3662.

[18] Todorov, T. K., Reuter, K. B., & Mitzi, D. B. (2010). High-Efficiency Solar Cell with Earth-Abundant Liquid-Processed Absorber. *Adv. Mater.*, *22*(20), E156-E159.

[19] Ito, S., Liska, P., Comte, P., Charvet, R., Péchy, P., Bach, U., Schmidt-Mende, L., Zakeeruddin, S. M., Kay, A., Nazeeruddin, M. K., & Grätzel, M. (2005). Control of Dark Current in Photoelectrochemical (TiO_2/I^--I^{3-})) and Dye-Sensitized Solar Cells. *Chem. Commun.*, *34*, 4351-4353.

[20] Knight, K. S. (1992). The Crystal Structures of $CuInSe_2$ and $CuInTe_2$. *Mater. Res. Bull.*, *27*, 161-167.

[21] Gobeaut, A., Laffont, L., Tarascon, J.-M., Parissi, L., Kerrec, O. (2009). Influence of Secondary Phases During Annealing on Re-crystallization of $CuInSe_2$ Electrodeposited Films. *Thin Solid Films*, *517*(15), 4436-4442.

[22] Nakada, T., Mizutani, M., Hagiwara, Y., & Kunioka, A. (2001). High-Efficiency Cu(In,Ga)Se_2 Thin-Film Solar Cells with a CBD-ZnS Buffer Layer. *Sol. Energy. Mater. Sol. Cells*, *67*(1-4), 255-260.

[23] Shafarman, W. N., & Zhu, J. (2000). Effect of Substrate Temperature and Depostion Profile on Evaporated Cu(InGa)Se_2 Films and Devices. *Thin Solid Films*, *361/362*, 473-477.

[24] Rahlfs, P. (1936). The Cubic High-Temperature Modifications of Sulfides, Selenides and Tellurides of Silver and of Univalent Copper. *Z. Phys. Chem. B*, *31*, 157-194.

[25] Gates, B., Yin, Y., & Xia, Y. (2000). A Solution-Phase Approach to the SYNTHesis of Uniform Nanowires of Crystalline Selenium with Lateral Dimensions in the Range of 10-30 nm. *J. Am. Chem. Soc*., *122*, 12582-12583.

[26] Paulson, P. D., Haimbodi, M. W., Marsillac, S., Birkmire, R. W., & Shafarman, W. N. (2002). $Cu(In_{1-x}Al_x)Se_2$ Thin Films and Solar Cells. *J. Appl. Phys*., *91*(12), 10153.

[27] Agilan, S., Managalaraj, D., Narayandass, S. K., & Rao, G. M. (2005). Effect of Thickness and Substrate Temperature on Structure and Optical Band Gap of Hot Wall-Deposited $CuInSe_2$ Polycrystalline Thin Films. *Physica B: Condensed Matter*, *365*(1-4), 93-101.

